International Journal of Minerals, Metallurgy and Materials
Volume 24, Number 1, January 2017, Page 1
DOI: 10.1007/s12613-017-1372-y

Mechanical properties and supporting effect of CRLD bolts under static pull test conditions

Xiao-ming Sun[1)], *Yong Zhang*[1)], *Dong Wang*[1,2)], *Jun Yang*[1)], *Hui-chen Xu*[1)], *and Man-chao He*[1)]

1) State Key Laboratory for Geomechanics and Deep Underground Engineering, China University of Mining and Technology, Beijing, Beijing 100083, China

2) State Key Laboratory of Mining Disaster Prevention and Control Co-founded by Shandong Province and the Ministry of Science and Technology, Shandong University of Science and Technology, Qingdao 266590, China

(Received: 2 June 2016; revised: 22 July 2016; accepted: 29 September 2016)

Abstract: A device for supporting soft rock masses combined with a constant resistance structure characterized by constant resistance and large deformation at the end of a steel bar, known as the constant resistance and large deformation (CRLD) bolt, has recently been developed to counteract soft rock swelling that often occurs during deep mining. In order to further study the mechanical properties of the CRLD bolt, we investigated its mechanical properties by comparison with the conventional strength bolt (rebar) using static pull tests on many aspects, including supporting capacity, elongation, radial deformation, and energy absorption. The tests verified that the mechanical defects of the rebar, which include the decrease of bolt diameter, reduction of supporting capacity, and emergence and evolution of fracture until failure during the whole pull process, were caused by the Poisson's ratio effect. Due to the special structure set on the CRLD bolt, the bolt presents a seemingly unusual phenomenon of the negative Poisson's ratio effect, i.e., the diameter of the constant resistance structure increases while under-pulling. It is the very effect that ensures the extraordinary mechanical properties, including high resistance, large elongation, and strong energy absorption. According to the comparison and analysis of numerical simulation and field test, we can conclude that the CRLD bolt works better than the rebar bolt.

Keywords: deep mining; bolts; mechanical properties; rock support; static pull test

1. Introduction

Under the conditions of high geostress and dynamic mining pressure in deep underground [1–2], the deformation of a soft rock roadway supported by conventional rebar bolts and cables is very large, which is mainly over 200 mm and sometimes more than 500 mm [3–5]. The large deformation will cause serious heaving of the floor, shrinking of the side walls, sinking of the roof, and potentially even roof collapse, definitely affecting normal use of roadway and mining safety [6–8]. The main reason for such phenomena is the Poisson's ratio that subjects the conventional rebar bolt or cable to low elongation and makes the bolt or cable unable to adapt when the surrounding rock deforms. When the conventional bolt/cable stretches due to the deformation of surrounding rock, it would exhibit the necking phenomenon, also known as the Poisson's ratio effect. Once the axial deformation exceeds the elongation limit, the conventional bolt/cable breaks and fails, which might finally lead to instability of roadway surrounding rock.

In view of the defects of the conventional supporting materials, many researchers have done some work on improving the elongation of the bolts. Examples include the cone bolt [9–10], modified cone bolt (with elongation no less than 180 mm) [11–12], Garford solid dynamic bolt [13], Roffex [14], D bolt (elongation as long as 400 mm) [15], and other types of energy-absorbing rock bolts [16–18]. These bolts could improve the properties of the conventional bolts to some extent, but the effect of Poisson's ratio still appears.

In 2014, He *et al.* [19] invented a bolt device, known as the constant resistance and large deformation (CRLD) bolt, which is combined with a constant resistance structure (CRS) characterized by constant resistance and large deformation

Corresponding author: Xiao-ming Sun E-mail: sxmcumtb@163.com

at the end of a steel bar CRLD bolt. It can provide high supporting resistance and large elongation, which can satisfy the soft rock roadway for large deformation [20–21].

In this paper, in order to study the mechanical properties of the CRLD bolt further, we first conducted pull tests on the CRLD bolt compared with the rebar bolt. Then, through data collection and results analysis, we finally summarized the extraordinary mechanical properties, especially, the negative effect of Poisson's ratio, of the CRLD bolt.

2. Experimental

2.1. Pull test in the laboratory

2.1.1. Materials

In this paper, four CRLD bolts and four rebar bolts were the subject of the static pull tests. The pictures of the CRLD and rebar bolts are shown in Figs. 1 and 2, respectively. The CRLD bolts comprise a CRS device and a connecting rod (Fig. 1(b)). The CRS device comprises a rod and sleeve pipe. The cone part of the rod is set in the inside of the sleeve pipe. The other end of the rod is the connecting part to fasten the connecting rod. The CRS device is the key structure that can provide the constant resistance during bolt stretching. The yield limit of the CRS device is lower than that of the connecting rod. The parameters of the chosen bolts are shown in Tables 1 and 2, respectively.

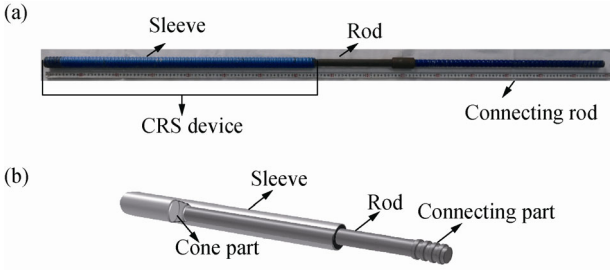

Fig. 1. CRLD bolt and its CRS device: (a) picture of the CRLD bolt; (b) schematic diagram of the CRS device.

Fig. 2. Rebar bolt.

Table 1. Parameters of the CRLD bolt

Bolt No.	Length / mm			Diameter / mm	
	Bolt	CRS device	Sleeve	Sleeve	Rod
CRLD-1	1586	1001	790	31.89	19.98
CRLD-2	1582	1002	788	31.93	20.02
CRLD-3	1584	1004	787	31.94	20.01
CRLD-4	1578	1003	788	31.89	19.99
Average	1581.25	1002.50	788.25	31.91	20.00

Table 2. Parameters of the rebar bolt

Bolt No.	Length of bolt / mm	Diameter of rod / mm
CRB-1	1578	19.42
CRB-2	1574	19.40
CRB-3	1582	19.46
CRB-4	1576	19.46
Average	1577.50	19.44

2.1.2. Test system

Pull tests in this paper adopt the LEW-500CRLD bolt/cable static pull test system, which comprises a main frame, a front collet component, a rear collet component, telescoping apparatus, and measurement and control apparatus, as shown in Fig. 3.

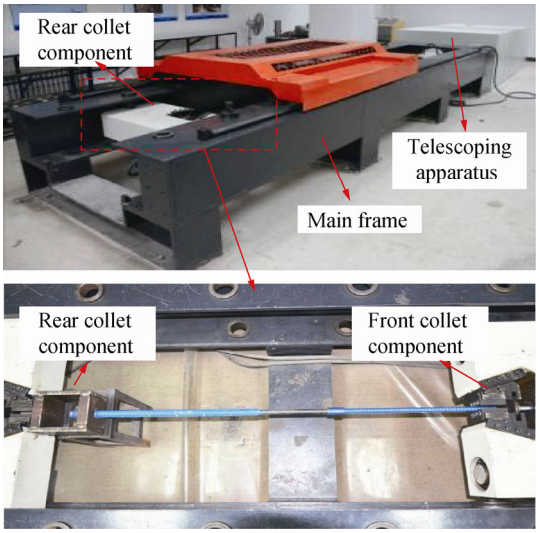

Fig. 3. LEW-500 CRLD bolt/cable static pull test system.

The basic parameters are shown as following: the maximum tensile load is 500 kN, the maximum measurement value is 1100 mm, the loading rate is 0.1–20 kN/min, the deformation rate is 0.5–100 mm/min.

2.1.3. Test method

Pull tests adopted the displacement control method with a closed loop. Before the pull tests, two groups of bolts were marked and measured piecewise. The measurement modes of the bolts are shown in Fig. 4. The distance between adjacent points is ten thread rings. Moreover, the diameter measurement uses reticle measurement in the direction of a–a and the direction of b–b. Measurement data include total length, segment length, and segment diameter before and after testing.

After the measurement work before testing, the connecting rod of the CRLD bolt is fixed by the front collet component. The other end of the bolt is connected to the rear

collet component by a special square device, as shown in Fig. 5(a). The rebar bolt is directly fixed by the front collet component and the rear collet component, as shown in Fig. 5(b).

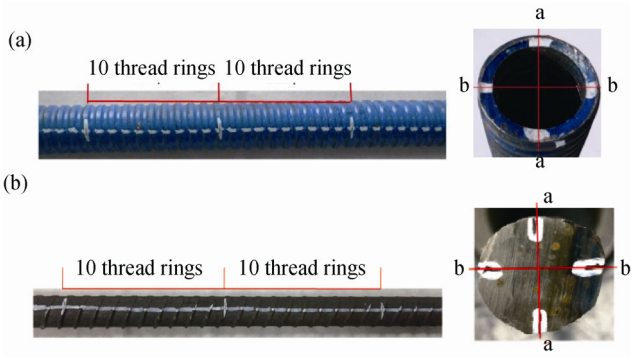

Fig. 4. Measurement modes of the bolts: (a) CRLD bolt; (b) rebar bolt.

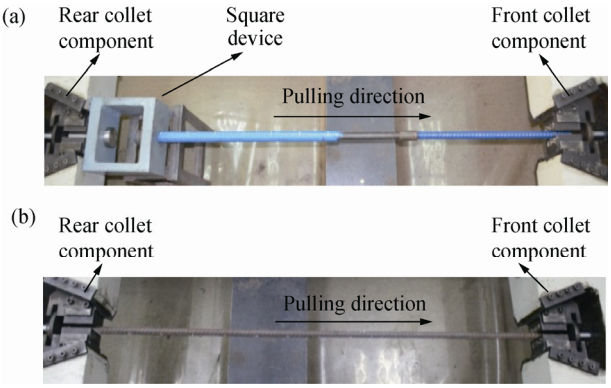

Fig. 5. Installation of the bolt during the pull test: (a) CRLD bolt; (2) rebar bolt.

The pull test system with uniform pull speed can automatically record the elongation, time, pull force, etc. When the rod of the CRLD bolt is pulled out from the sleeve pipe or the rebar bolt breaks, the pull test ceases. After the test, the corresponding data, including total length, segment length, and segment diameter should be measured.

2.2. Field test

For analyzing the supporting effects of CRLD bolt and rebar bolt, respectively, we conducted the comparative field tests at Xin'an Coal Mine, Gansu Province, China.

The field is located at the +535 air return crosscut, and the burial depth of the roadway is approximately 750 m. The location of the roadway in the strata and the lithology of the surrounding rock are shown in Fig. 6. The excavation process of the roadway mainly exposes fine sandstone and mudstone, and the roof and floor strata primarily comprise sandy mudstone, mudstone, fine sandstone, and coal.

Histogram	Depth / m	Elevation / m	Stratathickness / m	Lithology
	712.5	+572.5	20.0	Sandymudstone
	717.5	+547.5	5.0	Mudstone
	719.0	+546.0	1.5	Siltstone
	727.0	+538.0	8.0	Mudstone
	733.0	+532.0	6.0	Finesandstone
	735.0	+530.0	2.0	Mudstone
	736.5	+528.5	1.5	Siltstone
	739.5	+525.5	3.0	Mudstone
	742.0	+523.0	2.5	Coal
	744.5	+520.5	2.5	Mudstone
	750.5	+514.5	6.0	Finesandstone

Fig. 6. Distribution of the lithology of the surrounding rock.

The swelling probability of the roadway surrounding rock is very high. According to the results of X-ray diffraction and scanning electron microscopy analysis, the main mineral composition of each stratum of the +535 air return crosscut is clay. The average content is 54.5%, and the maximum content reaches to 61.75%. The clay minerals of each rock stratum mainly comprise kaolinite, followed by a ledikite–montmorillonite mix layer, ledikite, etc. Among that, the average content of kaolinite is 44%, and the maximum content reaches to 57%; the average content of the ledikite–montmorillonite mix layer is 39.6%, and the maximum content reaches to 44%; the average content of ledikite is 13.8%, and the maximum content reaches to 20%.

The distribution of test sections using different bolt support schemes is shown in Fig. 7. The total length of the +535 air return crosscut is approximately 700 m, mainly supported by the rebar bolts designed in the original support scheme before construction. We chose a length of 60 m of the +535 air return crosscut in the middle of the roadway to use the support scheme of the CRLD bolts so as to show the advantages over the original support scheme. In order to show the support effect, four monitoring points were arranged to monitor the deformation of surrounding rock and the stretch deformation of CRS device of the CRLD bolts.

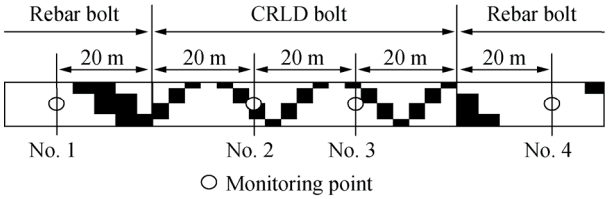

Fig. 7. Distribution of test sections.

The bolt support parameters of the roadway are the same with each other; only the type of supporting bolt is different (see Fig. 8). The numbers ranging from −5 to 5 represent the

bolt number. The inter-row space between bolts arranged on each cross-section is 750 mm.

3. Results and discussion

3.1. Static pull mechanical properties

3.1.1. Data analysis of pull test

From the pull load-deformation curves of the pull tests (Fig. 9), we can see the test results are very consistent between bolts with the same type (CRLD bolt or rebar bolt).

After measurements before and after the pull test, the test data of the CRLD bolts and rebar bolts are shown in Table 3 and 4, respectively.

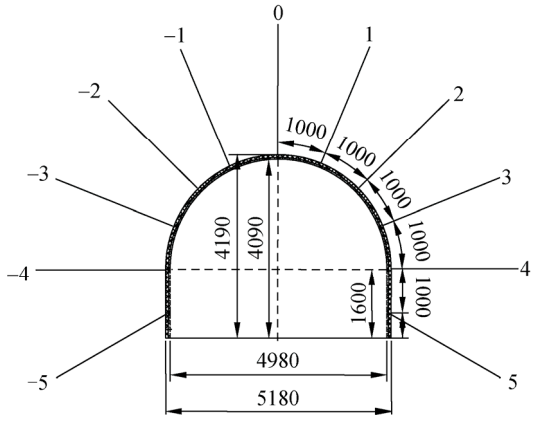

Fig. 8. Bolt support scheme (unit: mm).

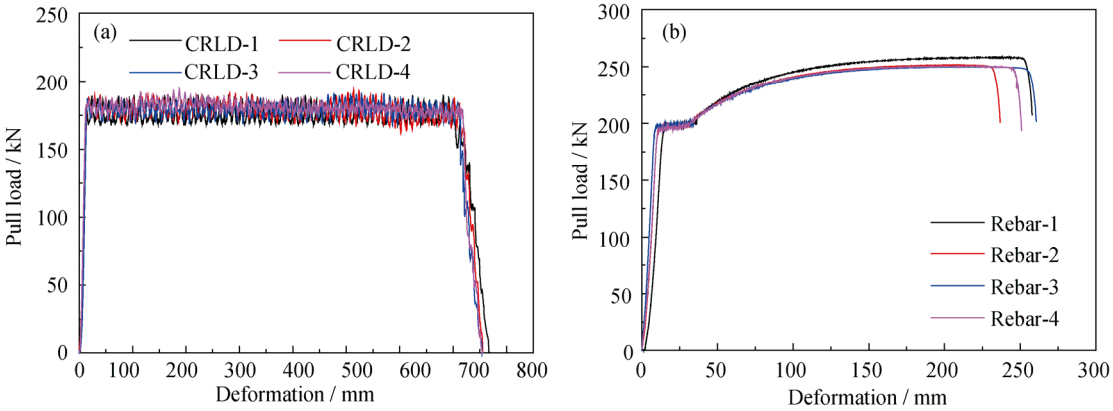

Fig. 9. Pull load–deformation curves in pull tests: (a) CRLD bolts; (b) rebar bolts.

Table 3. Test data of the CRLD bolt

Number of bolt	Pull load / kN			Fluctuation ratio	Deformation / mm		Elongation ratio
	Min.	Max.	Average		Sleeve	Total	
CRLD-1	167.85	189.18	176.14	+7.40% – −4.71%	16.20	760	47.92%
CRLD-2	161.80	193.60	178.52	+8.45% – −9.37%	14.60	755	47.72%
CRLD-3	167.70	190.70	179.47	+6.26% – −6.56%	15.32	754	47.60%
CRLD-4	171.10	194.30	181.00	+7.35% – −5.47%	16.16	756	47.91%
Average	167.11	191.95	178.78	+7.36% – −6.53%	15.57	756.25	47.79%

Table 4. Test data of the rebar bolt

Number of bolt	Yield pull load / kN	Max. pull load / kN	Total deformation / mm	Elongation ratio
Rebar-1	199.50	258.30	257.82	16.34%
Rebar-2	197.78	251.70	236.78	15.04%
Rebar-3	199.09	249.90	260.63	16.47%
Rebar-4	196.86	250.50	250.82	15.91%
Average	198.31	252.60	251.51	15.94%

The curve of the CRLD bolt (Fig. 10(a)) can be divided into three stages. At the beginning of the pull test, the CRLD bolt enters the first stage, in which the pull load increases quickly, and the CRLD bolt is in the stage of elastic deformation. Then, the pull load fluctuates within a small range (between approximately 23 to 31.80 kN) for a long time before reaching a certain value; we can call this stage the constant resistance deformation stage. Finally, when the rod is

pulled out from the sleeve pipe, the bolt enters the third stage, and the curve sees a dramatic drop from approximately 175 to 0 kN. The curve of the rebar bolt can be divided into four stages (Fig. 10(b)). In the first stage, the pull load increases to point A quickly. The rebar bolt is in the stage of elastic deformation just as with the CRLD bolt. In the second stage, the pull load maintains a stable value from point A to B. The rebar bolt is in the stage of yield deformation. In the third stage, both the pull load and stretch deformation increase from point B to C. The rebar bolt is in the plastic hardening stage. When the weak point of the bolt breaks, the pull force quickly drops to the fourth stage.

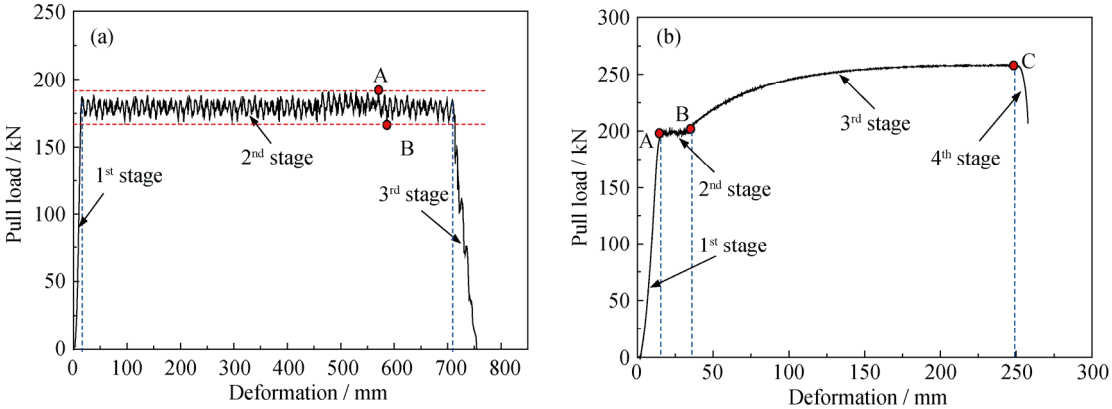

Fig. 10. Stage division of the pull deformation process: (a) CRLD bolts; (b) rebar bolts.

3.1.2. Constant resistance effect

During the pull test, the rebar bolts will be yielded when the pull load reaches the yield strength limit of the bolt material. The average yield pull load is approximately 198.31 kN. The rebar bolt cannot provide a constant resistance.

Although there is a little fluctuation of the pull load in the constant resistance deformation stage of the CRLD bolts compared to the conventional rebar bolts, it can be viewed as keeping a relative constant resistance for a large stretch deformation as long as the sleeve length. The average constant resistance is approximately 178.78 kN, which does not exceed the yield value of the bolt material. Therefore, the CRLD bolt is in the elastic stage of the material during the whole pull process. Obviously, the CRLD bolt has a unique property of high constant resistance effect.

3.1.3. Large elongation effect

Before the test, the average length of the CRLD bolts is 1581.25 mm, and the rebar bolts is 1522.50 mm. The difference between the two types of bolts is very narrow. The average elongation of the CRLD bolts is 756.25 mm, obviously longer than that of the rebar bolts with only 251.51 mm average elongation. Similarly, the average elongation ratio of the CRLD bolts (47.79%) is much higher than that of the rebar bolts (15.94%). Therefore, the CRLD bolts exhibit a large elongation effect.

A bolt can absorb the deformation energy of the surrounding rock through stretch deformation. Large elongation effect can provide a strong capacity of absorbing energy to the CRLD bolt.

3.1.4. Structural negative Poisson's ratio effect

Conventional materials often present necking phenomena when stretched or increasing transverse volume when compressed. Their Poisson's ratios are both positive. However, the materials with negative Poisson's ratio present lateral expansion. The unusual phenomenon of "stretch expansion" made the materials with negative Poisson's ratio become a new noteworthy material. In 1927, Love [22] discovered negative Poisson's ratio effect in pyritization. In 1987, Lakes [23] prepared foam material with negative Poisson's ratio. Subsequently, a series of materials with negative Poisson's ratio effect were designed in a rapid developmental stage of the unusual materials [24–25]. Evans *et al.* [26] denoted the materials or structure with negative Poisson's ratio "auxetics" and proposed that the materials had broad application prospects. In 2001, Yang *et al.* [27] summarized the unique property, classification, and microstructure of materials with negative Poisson's ratio. In 2001, Yang and Deng [28] reviewed the developmental process of research on the mechanical properties of materials and structures with negative Poisson's ratio, including the stretch expansion theory and the preparation and application of materials and structures with negative Poisson's ratio.

From monitoring data before and after the pull tests, the conventional rebar bolts showed the obvious Poisson's ratio effect. First, except the broken point, the diameter of monitoring points along the rebar bolt becomes smaller. To be specific, it changes from 19.4 to 17.62 mm in the a–a direc-

tion (Fig. 11(a)) and changes from 19.45 to 17.65 mm in the b–b direction (Fig. 11(b)). Second, we can clearly see the necking phenomena, from the high-speed photography (Fig. 12).

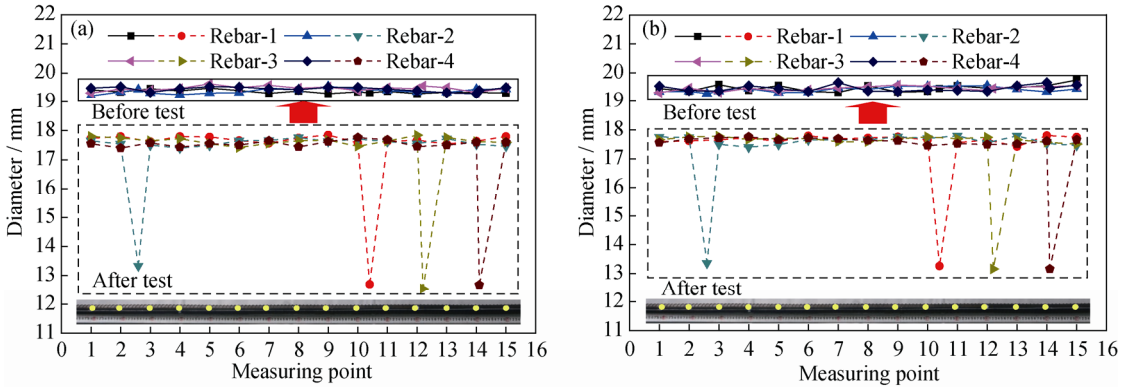

Fig. 11. Diameter variation of the rebar bolts before and after test: (a) in the a–a direction; (b) in the b–b direction.

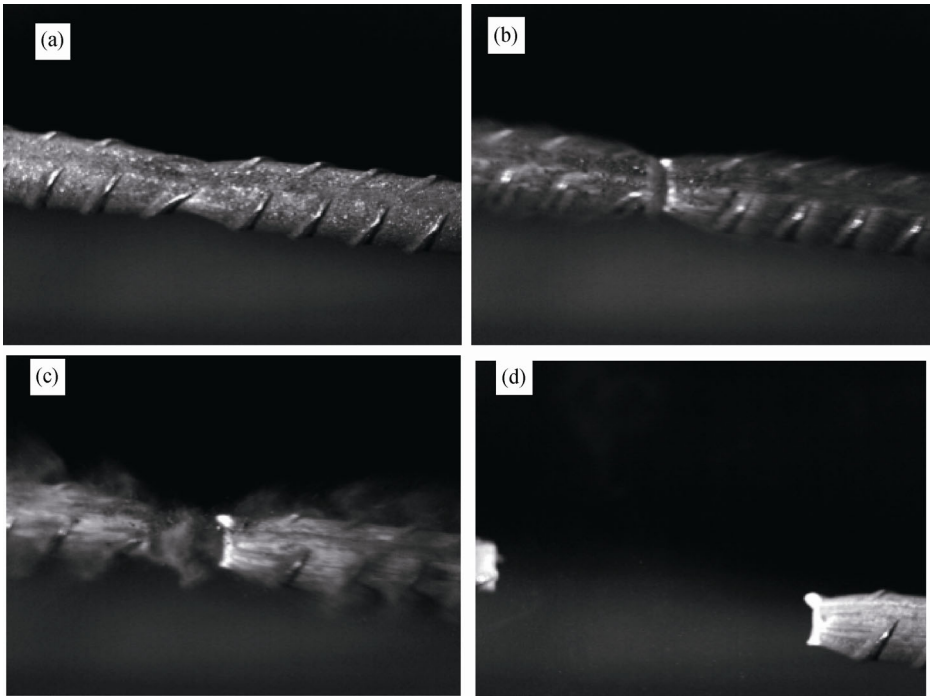

Fig. 12. High-speed photography of the rebar bolt necking phenomenon: (a) necking phenomenon; (b) plastic failure; (c) moment of tensile failure; (d) after tensile failure.

During the pull test of the CRLD bolt, there was a great different phenomenon in radial deformation. The diameter of the connected rod, which comprises the same type of material as the rebar bolt, did not change, but the CRS device showed the "stretch expansion" phenomenon. From monitoring data before and after the pull test, the sleeve diameter of the CRS device became larger, from 31.90 to 34.15 mm in the a–a direction (Fig. 13(a)) and from 31.92 to 34.13 mm in the b–b direction (Fig. 13(b)).

The reason for causing the "stretch expansion" phenomenon is the novel design of the CRS device (Fig. 13). During the pull process of the CRLD bolt, the cone part moves within the sleeve pipe. It is the movement of the rod that causes the elongation of the bolt. Due to the special structure of the cone part, the movement results in the expansion of the sleeve pipe, so the sleeve diameter after the pull test becomes larger.

The "stretch expansion" phenomenon matches the characteristic of negative Poisson's ratio, and it is caused by the structure of the CRLD bolt, so we can consider it structural negative Poisson's ratio effect. And it is the property of structural negative Poisson's ratio effect that ensures the constant resistance effect and large elongation effect of the CRLD bolt.

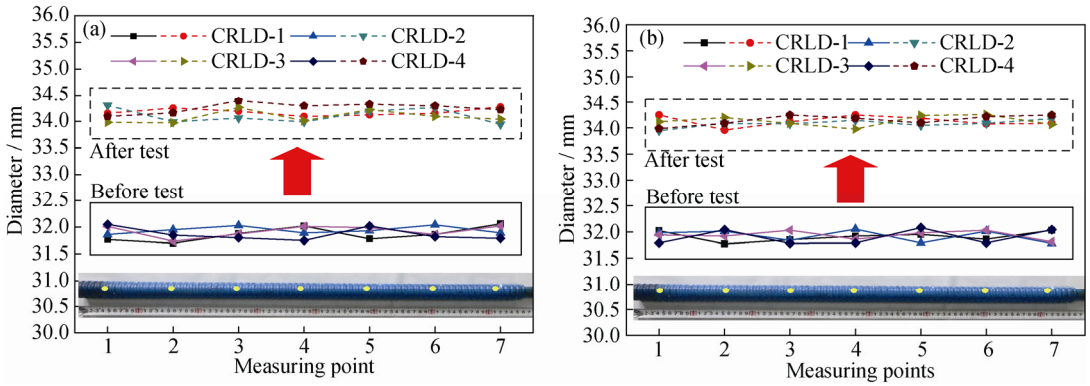

Fig. 13. Diameter variation of the sleeve of the CRLD bolt before and after test: (a) in the a–a direction; (b) in the b–b direction.

3.1.5. Theoretical model of CRLD bolts

The relationship between elongation and load of the rebar bolt can be divided into four stages, i.e. elastic stage, yielding stage, strengthening stage and local deformation stage. The rebar bolt will begin to lose the support strength in practical engineering when it reaches to the yielding stage. However, the form of resistance of the CRLD bolt can be written as [19]

$$P_0 = 2\pi f I_s I_c \tag{1}$$

where P_0 is the overall resistance, f is the frictional coefficient, I_s is the sleeve elastic constant, and I_c is the cone geometrical constant.

I_s can be written by

$$I_s = \frac{E(b^2 - a^2)\tan\alpha}{a[a^2 + b^2 - \mu(b^2 - a^2)]} \tag{2}$$

I_c can be written by

$$I_c = \frac{ah^2}{2}\cos\alpha + \frac{h^3}{3}\sin\alpha \tag{3}$$

where a is the inner radius of the sleeve, b is the outer radius of the sleeve, α is the cone angle; h is the height of the cone part, E is the elastic modulus, and μ is the Poisson's ratio.

Based on a series of theoretical analyses [19], the constitutive relation for the CRLD bolt can be written as

$$P = \begin{cases} kx, & 0 \leqslant x \leqslant x_0, \quad P < P_{\max} \quad \text{(elastic deformation)} \\ P_{\max} - P_{\min} = k\Delta x, & x > x_0 \quad \text{(stick-slipping motion)} \end{cases} \tag{4}$$

From Eqs. (1)–(4), we can see that the CRLD bolt has no yield strength which is an important characteristic of the CRLD bolt.

3.2. Supporting effect

The field test results are shown in Fig. 14. Compared with two types of bolt support, the deformation of roadway surrounding rock with the rebar bolts is much larger than that with the CRLD bolt. It indicates that the rebar bolt support could not bear the large deformation of surrounding rock (Fig. 15(a)). According to the laboratory observations (Figs. 15(b) and (c)), we find that some rebar bolts occurred necking phenomena and broke. Figs. 16 (a) and (b) are the CRS device deformation curves of the CRLD bolt support. It shows that the large elongation effect of the CRLD bolt ensures the CRLD bolt stretching during the process of large deformation of roadway surrounding rock, and avoids being broken. What is more, the high constant resistance effect can

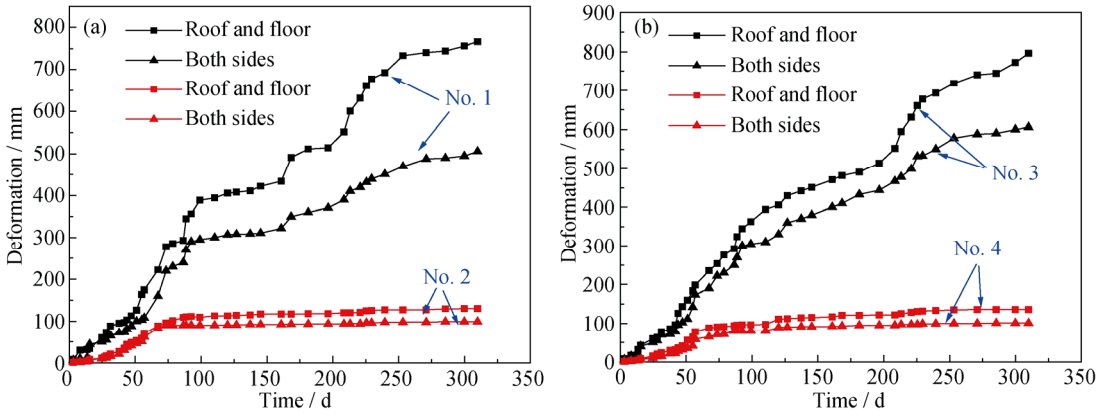

Fig. 14. Deformation curves of roadway surrounding rock: (a) monitoring points of No.1 and No. 2; (b) monitoring points of No. 3 and No. 4.

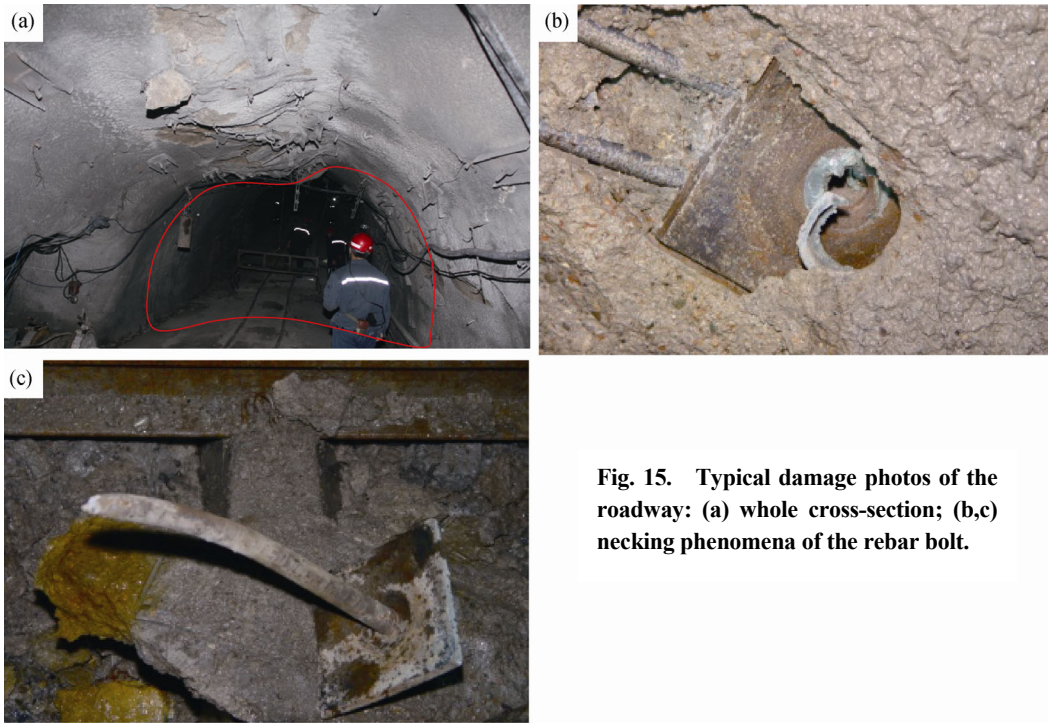

Fig. 15. Typical damage photos of the roadway: (a) whole cross-section; (b,c) necking phenomena of the rebar bolt.

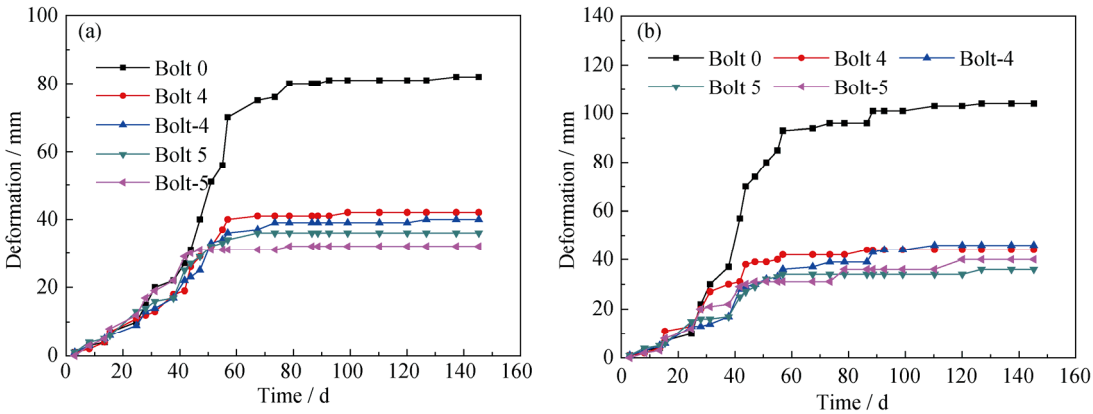

Fig. 16. Deformation of the CRS device of the CRLD bolts: (a) cross-section of No. 2; (b) cross-section of No. 3.

realize the controlled release of deformation energy of surrounding rock, so the supporting effect of the CRLD bolt can satisfy the stability of the soft rock roadway more than that of the rebar bolt (Fig. 17).

Fig. 17. Supporting effect of the CRLD bolt.

4. Conclusions

The results verified that the mechanical defects of the conventional rebar bolt, including the decrease of bolt diameter, the reduction of supporting force, and the development of fracture until total failure during the pull process, were caused by Poisson's ratio effect.

Due to the unique structure of the new-type bolt, the CRLD bolt shows the seemingly unusual phenomenon of negative Poisson's ratio effect, which means that the increase of bolt diameter and also ensures the unique mechanical properties, including high constant resistance, extraordinary elongation and strong energy absorption.

Compared with the CR bolt, the CRLD bolt can positively control the development of deformation of the roof

and side walls by the controlled release of stress accumulated in swelling soft rock. It is advantageous to keep the integrity of roadway surrounding rock and the performance of the CRLD bolt support system to ensure the stability of the roadway.

Acknowledgements

This work was supported by National Key Research and Development Program (2016YFC0600901), the National Natural Science Foundation of China (Grant Nos. 51374214, 51134005 and 51574248), the Special Fund of Basic Research and Operating of China University of Mining & Technology, Beijing (Grant Nos. 2009QL03), and the State Scholarship Fund of China.

References

[1] M.C. He, H.P. Xie, S.P. Peng, and Y.D. Jiang, Study on rock mechanics in deep mining engineering, *Chin. J. Rock. Mech. Eng.*, 24(2005), No. 16, p. 2803.

[2] M.C. He, Latest progress of soft rock mechanics and engineering in China, *J. Rock Mech. Geotech. Eng*., 6(2014), No. 3, p. 165.

[3] C. Fairhurst, Deformation, yield, rupture and stability of excavations at depth in rock, [in] D. Fourmaintraux and V. Maury, *Rock at Great Depth*, Balkema, Rotterdam, 1989, p. 1103.

[4] M.C. He and X.M. Sun, *China Coal Mine Soft Rock Engineering Supporting Design and Construction Guide*, Science Press, Beijing, 2004, p. 109.

[5] M.C. He, H.H. Jing, and X.M. Sun, *Soft Rock Engineering Mechanics*, Science Press, Beijing, 2002, p. 6.

[6] X.M. Sun, G.F. Zhang, F. Cai, and S.B. Yu, Asymmetric deformation mechanism within inclined rock strata induced by excavation in deep roadway and its controlling countermeasures, *Chin. J. Rock. Mech. Eng.*, 28(2009), No. 6, p. 1137.

[7] X.M. Sun, D. Wang, J.L. Feng, C. Zhang, and Y.W. Chen, Deformation control of asymmetric floor heave in a deep rock roadway: a case study, *Int. J. Min. Sci. Technol.*, 24(2014), No. 6, p. 799.

[8] H.P. Kang, J.H. Wang, and J. Lin, Case studies of rock bolting in coal mine roadways, *Chin. J. Rock Mech. Eng.*, 29(2010), No. 4, p. 649.

[9] A.J. Jager, Two new support units for the control of rockburst damage, [in] P.K. Kaiser and D.R. McCreath, *Rock Support in Mining and Underground Construction*, Balkema, Rotterdam, 1992, p. 621.

[10] L. St-Pierre, F.P. Hassani, P.H. Radziszewski, and J. Ouellet, Development of a dynamic model for a cone bolt, *Int. J. Rock Mech. Min. Sci.*, 46(2009), No. 1, p. 107.

[11] C.C. Li and P.I. Marklund, Field tests of the cone bolt in the Boliden mines, [in] *Annual Meeting of Rock Mechanics*, Stockholm, 2005, p. 33.

[12] M. Cai, Principles of rock support in burst-prone ground, *Tunnelling Underground Space Technol.*, 36(2013), p. 46.

[13] R. Varden, R. Lachenicht, J.R. Player, A.G. Thompson, and E. Villaescusa, Development and implementation of the Garford dynamic bolt at the Kanowna Belle mine, [in] *10th Underground Operators Conference*, Launceston, Aus IMM, Melborune, 2008, p. 95.

[14] F. Charette and M. Plouffe, A new rock bolt concept for underground excavations under high stress conditions, [in] *Sixth International Symposium on Ground Support in Mining and Civil Engineering Construction*, SAIMM, Johannesburg, 2008, p. 225.

[15] C.L. Charlie, A new energy-absorbing bolt for rock support in high stress rock masses, *Int. J. Rock Mech. Min. Sci.*, 47(2010), No. 3, p. 396.

[16] C.J. Hou and Y.N. He, Principle and application of rockbolts with extensible rod, *Chin. J. Rock Mech. Eng.*, 16(1997), No. 6, p. 544.

[17] D.D. Tannant and B.W. Buss, Yielding rockbolt anchors for high convergence or rockburst conditions, [in] *Proceedings of the 47th Canadian Geotechnical Conference*, Halifax, 1994, p. 10.

[18] A. Ansell, Laboratory testing of a new type of energy absorbing rock bolt, *Tunnelling Underground Space Technol.*, 20(2005), No.4, p. 291.

[19] M.C. He, W.L. Gong, J Wang, P. Qi, Z.G. Tao, S. Du, and Y.Y. Peng, Development of a novel energy-absorbing bolt with extraordinarily large elongation and constant resistance, *Int. J. Rock Mech. Min. Sci.*, 67(2014), p. 29.

[20] M.C. He and Z.B. Guo, Mechanical property and engineering application of anchor bolt with constant resistance and large deformation, *Chin. J. Rock Mech. Eng.*, 33(2014), No.7, p. 1297.

[21] X.M. Sun, D. Wang, C. Wang, X. Liu, B. Zhang, and Z.Q. Liu, Tensile properties and application of constant resistance and large deformation bolts, *Chin. J. Rock Mech. Eng.*, 33(2014), No. 9, p. 1765.

[22] A.E.H. Love, *A Treatise on the Mathematical Theory of Elasticity*. 4th Ed., Cambridge University Press, Cambridge, 1927, p. 68.

[23] R. Lakes, Foam structures with a negative Poisson's ratio, *Science*, 235(1987), p. 1038.

[24] E.A. Friis, R.S. Lakes, and J.B. Park, Negative Poisson's ratio polymeric and metallic foams, *J. Mater. Sci.*, 23(1988), No. 12, p. 4406.

[25] M.A. Loureiro and R.S. Lakes, Scale-up of transformation of negative Poisson's ratio foam: slabs, *Cell. Polym.*, 16(1997), No. 5, p. 349.

[26] K.E. Evans, M.A. Nkansah, and I.J. Hutchinson, and S.C. Rogers, Molecular network design, *Nature*, 353(1991), No. 6340, p. 124.

[27] M.B. Yang, X. Yang, Z.M. Li, and J.M. Feng, The structure and properties of the material with negative Poisson's ratio, *Polym. Mater. Sci. Eng.*, 17(2001), No. 6, p. 15.

[28] Z.C. Yang and Q.T. Deng, Mechanical property and application of materials and structures with negative Poisson's ratio, *Adv. Mech.*, 41(2011), No. 3, p. 335.